(Received 21 August 2025, Accepted 15 November 2025, Scheduled 29 November 2025)

Optimization of Multilayer Microwave Absorbers Using Hybrid Multi-Strategy Improved Enzyme Action Optimizer

Tongyu Liu[1], Weibin Kong[1, 3, *], Yiming Zong[1], Lei Wang[1, *], Yuanyuan Wang[1], Wenwen Yang[2], and Yidong Wei[1]

[1] *School of Information Engineering, Yancheng Institute of Technology, Yancheng, China*
[2] *School of Science and Technology, Nantong University, Nantong 226019, China*
[3] *State Key Laboratory of Millimeter Waves, Southeast University, Nanjing 210096, China*

ABSTRACT: This paper proposes a Hybrid Multi-Strategy Enhanced Enzyme Action Optimizer (HSEAO) for designing multilayer broadband microwave absorbers under vertical irradiation conditions. The optimization objective is to minimize the absorber's reflection coefficient within a specified frequency range by selecting suitable material layers from a literature database. The performance of the Enzyme Action Optimizer (EAO) has been improved by introducing three enhancement strategies including Quasi-Opposition Based Learning (QOBL), adaptive coefficient, and leader follower. The effectiveness of these enhancement strategies is validated through simulation examples of five-layer and seven-layer microwave absorbers, achieving maximum reflection losses of -25.7975 dB and -18.1965 dB, respectively. Results demonstrate that HSEAO outperforms other heuristic algorithms in minimizing reflection coefficients for microwave absorber design. CST simulations further demonstrate that microwave absorbers designed by HSEAO achieve lower reflection losses.

1. INTRODUCTION

Microwave absorbers are functional materials that effectively absorb microwave energy incident on their surfaces and dissipate most of it as thermal energy or other forms of energy. Their primary objective is to minimize reflection, maximize absorption, and suppress transmission. Their operating principle primarily relies on dielectric loss and magnetic loss within the material, achieving impedance matching to maximize electromagnetic wave penetration into the material, and utilizing destructive interference effects to reduce reflection [1]. As electromagnetic environments become increasingly complex, the demand for lightweight, high-performance microwave absorption materials continues to grow. Compared to single-layer absorbers, multi-layer structured absorbers not only broaden the absorption bandwidth and enhance absorption efficiency but also offer greater design flexibility and complementary material properties [2]. They are widely applied in fields such as stealth technology [3], electromagnetic compatibility [4], microwave anechoic chambers [5], and electronic device protection [6].

In the event of vertical incidence, the optimization of multilayer microwave absorbers (MMA) focuses on three major areas: impedance matching optimization, loss mechanism enhancement, and structural parameter design. From an engineering standpoint, the process of selecting suitable materials and precisely adjusting their layer thicknesses to suppress the reflection coefficient across the desired frequency band forms a crucial foundation for developing an effective optimization scheme. Based on this, intelligent optimization algorithms emerge as the optimal solution for addressing such challenges.

A method based on genetic algorithm for synthesizing multilayer radar absorbing coatings has been proposed by Michielssen et al., which determined the selection of materials for each layer and its thickness [7]. With the emergence of more heuristic algorithms, an increasing number of such algorithms have been successfully applied in the design of MMA. Examples include particle swarm optimization (PSO) and related optimization algorithms [8, 9], differential evolution (DE) [10], cuckoo search algorithm (CSA) [11], blended algorithm of simulated annealing and simulated annealing (BLSA-SA) [12], bald eagle search optimization algorithm (BESOA) [13], multi-strategy improved gold rush optimizer (MIGRO) [14] and improved estimation of distribution algorithm (IEDA) [15]. Based on extensive experimental comparisons and analyses, there is still room for further development of the algorithm in global search capabilities and convergence to the performance of MMA.

In this study, HSEAO, thanks to its excellent global search capabilities and convergence speed, is proposed to determine the optimal pairing of layer sequence and corresponding thickness for the design of MMA. In order to improve the convergence rate and global exploration ability of HSEAO, three enhancement strategies were employed, including QOBL, adaptive coefficients, and leader-follower strategy. Two design examples demonstrate that, compared to other heuristic algorithms, HSEAO yields improved reflection coefficients in the design of MMA, thereby enhancing the absorptive capabilities of the optimized materials. Moreover, the reliability of both

* Corresponding authors: Weibin Kong (kongweibin2007@sina.com); Lei Wang (wanglei_ntu@outlook.com).

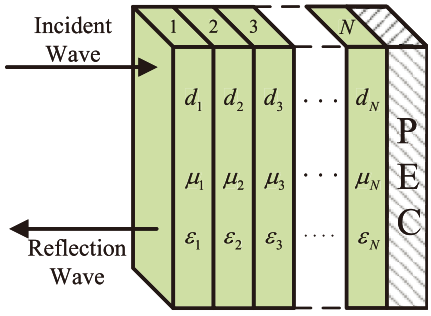

FIGURE 1. Physical model of MMA.

designs has been verified through Computer Simulation Technology (CST) full-wave simulation.

2. PHYSICAL MODEL OF MULTILAYER ABSORBER

Figure 1 presents the physical model used to describe the structure of the microwave absorber, where a uniform plane wave is incident normally on its surface. This absorber comprises N planar layers backed by a Perfect Electric Conductor (PEC). Each layer that making up the absorber has a different thickness, and the magnetic/electrical properties of each layer vary significantly depending on the frequency. The thickness, dielectric constant, and magnetic permeability of each layer are denoted by d_i, μ_i, and ε_i, respectively. According to the equivalent transmission line theory of electromagnetic waves, this structure can be represented as a circuit model composed of cascaded N-segment uniform transmission lines [16, 17], as shown in Fig. 2.

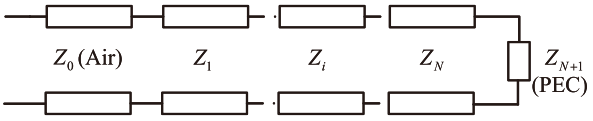

FIGURE 2. Equivalent circuit diagram of MMA.

In this model, the loss value returned by the calculation is used as the standard to evaluate the electromagnetic wave absorption performance of the MMA, expressed as an equation, and serves as the objective function for optimization:

$$F_{\text{loss}} = 20\log_{10}(\max|R|) \tag{1}$$

where R represents the reflection coefficient at the boundary between free space and the absorbing medium. It is calculated by the formula:

$$R = \frac{Z_1 - Z_{\text{free}}}{Z_1 + Z_{\text{free}}} \tag{2}$$

where Z_{free} is the intrinsic impedance of free space. The total impedance of the absorber is described as Z_1. In the case of direct incidence, the input impedance Z_i of the corresponding layer can be described as follows:

$$Z_i = \eta_i \frac{Z_{i+1} + j\eta_i \tan(\beta_i d_i)}{\eta_i + jZ_{i+1}\tan(\beta_i d_i)}, \quad i < N \tag{3}$$

As for the input impedance of layer N, it is equivalent to the input impedance of a transmission line with a short-circuit termination, which is expressed as follows:

$$Z_i = j\eta_i \tan(\beta_i d_i), \quad i = N \tag{4}$$

where β_i, d_i, and η_i are the phase constant, thickness, and wave impedance of the corresponding ith layer. η_i and β_i are defined separately as follows:

$$\eta_i = \sqrt{\frac{\mu_i}{\varepsilon_i}} \tag{5}$$

$$\beta_i = \frac{2\pi f}{c}\sqrt{\varepsilon_{r,i}\mu_{r,i}} \tag{6}$$

where μ_i and ε_i represent the magnetic permeability and dielectric constant of each layer's material; $\mu_{r,i}$ and $\varepsilon_{r,i}$ denote the relative magnetic permeability and relative permittivity; f is the operating frequency; and c donates the speed of light in a vacuum.

Designing MMA constitutes a nonlinear multivariate optimization problem that requires consideration not only of continuous variables such as thickness and frequency, but also of discrete variables like different coating combinations. Thickness must account for not only the overall thickness constraints of the absorber, but also the specific thickness of each individual coating layer.

3. ENZYME ACTION OPTIMIZER

3.1. Basic Enzyme Action Optimizer

Enzyme Action Optimizer (EAO) is a novel bio-inspired optimization algorithm that mimics the catalytic mechanisms of biological enzymes. It effectively balances exploration and exploitation, enabling efficient navigation through high-dimensional and complex search spaces. This is accomplished by simulating the dynamic interactions between enzymes and substrates [18]. Enhanced diversity through random difference vectors and cofactors initially (exploration), and optimization through optimal solution steering and local perturbation focus later (exploitation). Its outstanding global search capability and convergence speed align well with the multi-parameter, multi-objective optimization requirements of absorbers.

The goal of the exploration process is to search extensively across the solution space, avoiding getting stuck in local optima while discovering potentially promising regions. This corresponds to the process of enzymes randomly binding to different substrates in the early stages, enhancing diversity. The core mechanisms are differential vector generation and candidate solution 2 generation.

$$d = X_p^{(t-1)} - X_q^{(t-1)} \tag{7}$$

where d is the positional difference between two different substrates p and q, used in the early stages of iteration to avoid premature convergence.

The key parameter adaptive factor AF is used to regulate the two stages of exploration and exploitation, and is expressed as:

$$AF = \sqrt{\frac{t}{MaxIter}} \tag{8}$$

The process of exploration is expressed as:

$$X_{i,2}^{(t)} = X_i^{(t-1)} + sc_1 \cdot d + AF_t \cdot sc_2 \cdot X_{best}^{(t-1)} - X_i^{(t-1)} \quad (9)$$

where *MaxIter* is the maximum number of iterations, and sc_1 and sc_2 are both random vectors, generated independently for each dimension, with values ranging from [0, 1].

The purpose of the exploitation process is to conduct a detailed search in the potential optimal region and accelerate convergence to the global optimal solution. The simulated enzyme forms a stable complex with the substrate, lowering the reaction energy barrier through fine-tuning of the active site. The mathematical expression for this process is:

$$X_{i,1}^{(t)} = \left(X_{best}^{(t-1)} - X_i^{(t-1)}\right) + \rho_i \cdot \sin\left(AF_t \cdot X_i^{(t-1)}\right) \quad (10)$$

where ρ_i is a random vector between 0 and 1. Sine high-frequency disturbances are introduced, and a fine search is performed in the vicinity of the optimal solution. AF_t is used to enhance the amplitude of the sine term and focus on local optimization.

In the basic EAO, the simple random selection of the initial population and the fixed index easily lead to insufficient population size and premature convergence. To address these issues, we selected three improvement measures to apply in the improved EAO.

3.2. Improved Enzyme Action Optimizer

In the basic EAO, the population is generated through random initialization, which may result in an uneven distribution of initial solutions. The QOBL is introduced in the initialization stage to enhance the diversity and search efficiency of the population by generating and utilizing "quasi-opposite solutions" [19]. A quasi-opposite solution x^{qo} is a random interpolation solution between the original solution and the completely opposite solution. Its mathematical definition is:

$$x^{qo} = x + r \cdot (x^{op} - x) \quad (11)$$

where x is the original solution, x^{op} the opposition solution, and r a random number between 0 to 1. After introducing the QOBL, the initial population simultaneously includes both the original solutions and better quasi-reverse solutions, achieving the goal of generating a high-quality population that covers the potential optimal region. During the iterative phase, for each iteration, a quasi-reverse solution is generated for each individual as a candidate position, competing with candidate solutions generated by other strategies. The better solution is selected to update the population, helping the algorithm escape the current local optimal region and enhancing its exploration capability.

To prevent premature convergence of the algorithm, we introduce an adaptive coefficient strategy. To ensure diversity in the number of iterations at different values, the weight coefficient ω is always set within the range [0, 1]. The mathematical logic in the original expression needs to be corrected, and its numerical stability under different scales of iterations needs to be verified. In the original case, there are problems of iteration variable exceeding the limit and insufficient numerical accuracy. The main improvement strategies are to adjust the exponential growth rate and replace the exponential with a linear approximation [20]. When *MaxIter* is less than 1000, ω is expressed as:

$$\omega = rand(\,) \times \left(1 - \frac{e^{\alpha \cdot t/MaxIter} - 1}{e^{\alpha} - 1}\right) \quad (12)$$

where α is a regulating factor, with a default value of 1, and *rand*( ) is a uniformly distributed random number. When *MaxIter* is very large, a Taylor expansion is used for approximation, linearizing ω with the expression given by:

$$\omega_{liner} = rand(\,) \times \left(1 - \frac{t}{MaxIter}\right) \quad (13)$$

The paper [21] introduces a bio-inspired algorithm based on the migratory behavior of humpback whales. The core of the algorithm is to simulate the cooperative behavior of humpback whale groups during migration. The article mentions a leader-follower strategy. Combined with adaptive coefficients, this strategy enhances the local search capability of the algorithm by selecting candidate batches and comparing their optimal solutions with each other. After integrating this strategy with EAO, the mathematical expression is:

$$\delta = \delta_0 \cdot \left[1 - \left(\frac{t}{MaxIter}\right)^2\right] \quad (14)$$

$$EC^{qo} = EC + rand \cdot (1 - EC) \quad (15)$$

$$\Delta x_{leader} = \delta \cdot EC^{qo} \cdot AF \cdot (g_{best} - x_i) \quad (16)$$

where δ is time-varying leadership influence factors, δ_0 a free variable between 0.3 and 0.7, and g_{best} the current global optimal solution.

The flowchart of HSEAO is shown in Fig. 3.

4. SIMULATION EXPERIMENT AND RESULT ANALYSIS

4.1. Simulation Experiment

For the multi-layer absorber physical model used in this experiment, the microwave reflection suppression is decided by the electromagnetic properties of each layer, the thickness and sequence of the layers, as well as the incident frequency of the electromagnetic wave. At the initialization stage, the thickness and material of each layer are initially assigned at random, and there are restrictions on the number of layers, maximum thickness, and bandwidth. Furthermore, the number of design variables equals twice the number of layers. The optimization process seeks to find the best combination of material types and layer thicknesses to achieve the lowest possible peak reflection coefficient.

The core of the optimization strategy lies in selecting the most suitable materials from a pre-established material database. In this work, the database includes 16 distinct materials, which are classified into four categories based on their electromagnetic properties: lossless dielectric materials,

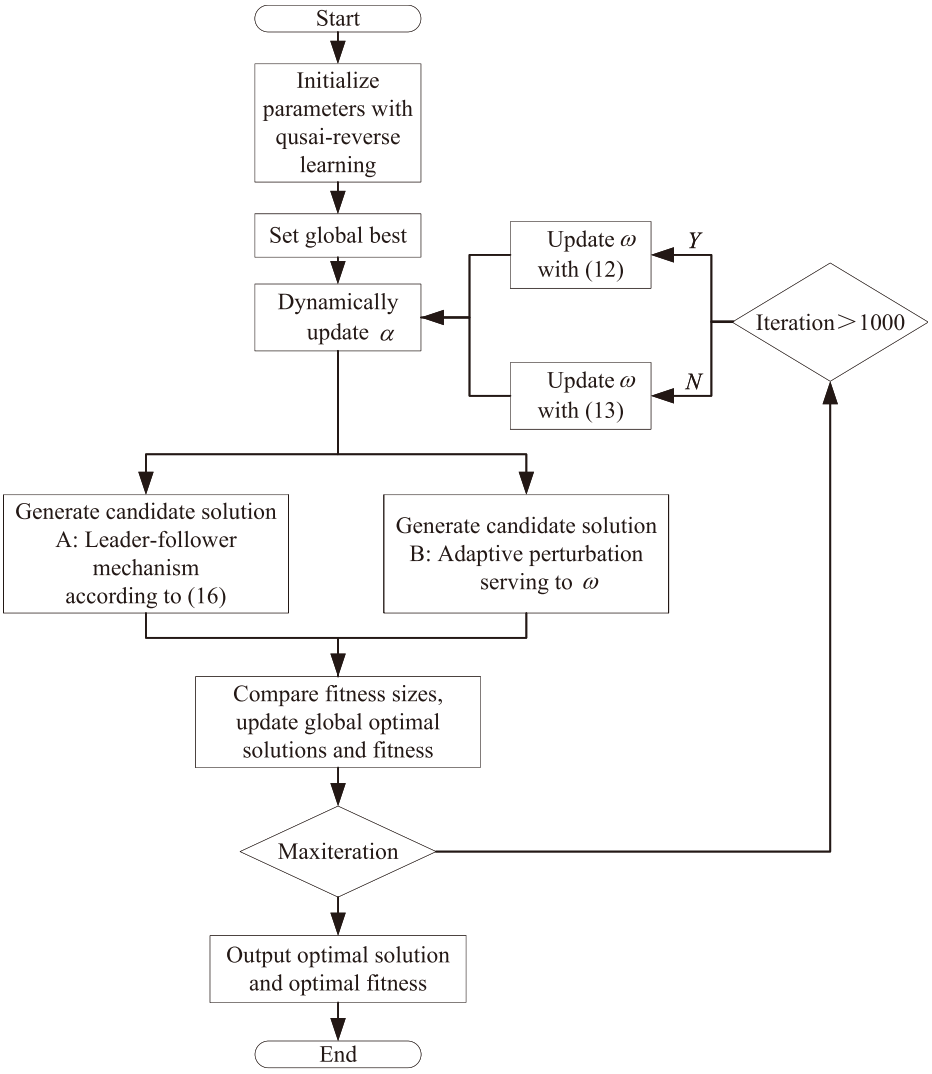

FIGURE 3. Flowchart of HSEAO.

lossy magnetic materials, lossy dielectric materials, and relaxor magnetic materials. The relative permittivities and magnetic permeabilities of these materials are listed in Table 1. This material library has been applied in multiple studies on the design of MMA [10, 12–14]. Additionally, the optimal design parameters — such as the material type and thickness of each layer — derived from other algorithms in the literature were used to compute the reflection coefficient across the specified frequency range. In this range, both the peak reflection coefficient and the overall reflection curve closely match the results reported in [7–14], indicating that the experimental simulations described below are reliable.

This section presents two design examples to illustrate the advantages of HSEAO in designing MMA. The HSEAO results are compared with standard EAO results and other heuristic algorithms published in the literature.

The mathematical modeling and optimization process of MMA materials was implemented using MATLAB R2024A software. The optimal material types and corresponding layer thicknesses obtained from numerical optimization are imported into CST for electromagnetic simulation. CST Studio Suite is a widely used 3D electromagnetic simulation tool that facilitates the validation of optimization results. This seamless workflow between MATLAB and CST ensures both computational efficiency and physical reliability [22].

4.2. Result Analysis

4.2.1. First Example: Five-Layer Absorber

This five-layer absorber is intended to function across the 2–8 GHz frequency band, with an interval of 0.1 GHz and a maximum total thickness limited to 5 mm. For both HSEAO and EAO, the population size is assigned as 20 with 1000 iterations. Each algorithm was independently executed 20 times to ensure statistical reliability. The comparison results with other literature [10, 12, 13] are presented in Table 2. The current experimental results are compared with coefficient curve within the frequency range, demonstrating the reliability of the experimental simulations presented below.

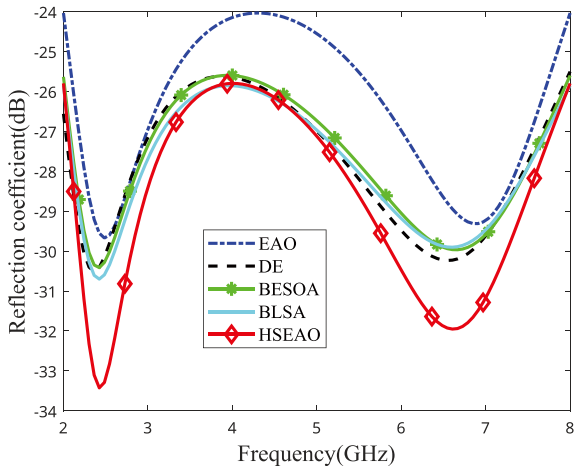

FIGURE 4. Comparison of reflection losses for five-layer absorber designs in the 2–8 GHz, frequency interval is 0.1 GHz.

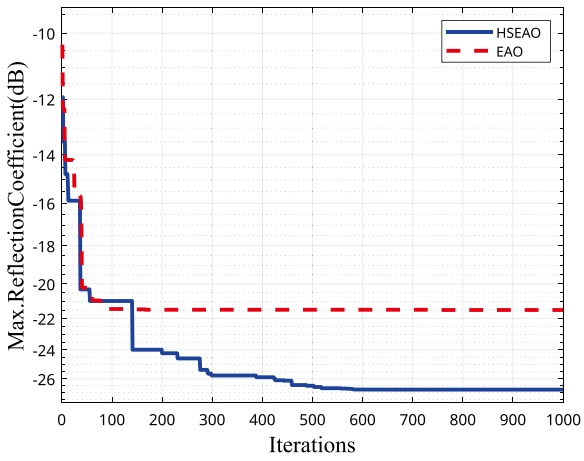

FIGURE 5. Comparison of convergence curves for five-layer designs.

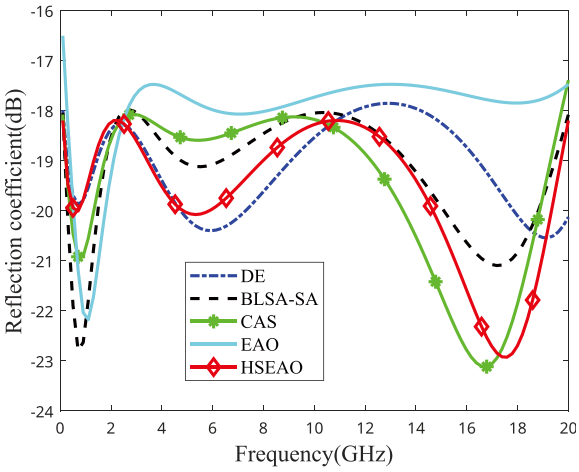

FIGURE 6. Comparison of reflection losses for seven-layer absorber designs in the 0.1–20 GHz, frequency interval is 0.1 GHz.

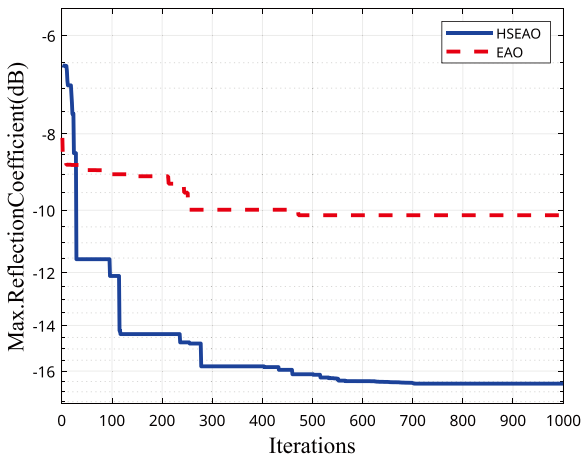

FIGURE 7. Comparison of convergence curves for seven-layer designs.

Comparative analysis of the test outcomes indicates that HSEAO attains the broadest absorption bandwidth within the 2–8 GHz frequency range, while sustaining the lowest mean reflection coefficient. Specifically, HSEAO attains a minimum reflection loss of −33.4237 dB at 2.48 GHz, as depicted in Fig. 4. Furthermore, Fig. 5 depicts that HSEAO demonstrates superior convergence accuracy during iterations compared to EAO, highlighting its enhanced optimization performance.

4.2.2. Second Example: Seven-layer Absorber

In this case, the design of the seven-layer absorber was carried out with a maximum total thickness of 10 mm. To comprehensively evaluate its performance, the absorption frequency range was expanded to 0.1–20 GHz. All other experimental parameters remained consistent with those of the five-layer model.

Results of HSEAO were compared with those data from [10–12]. As shown in Table 3, HSEAO achieved the lowest maximum and average reflection losses of −18.20 dB and −19.64 dB, respectively.

It also had the widest frequency band coverage, demonstrating excellent broadband absorption capabilities. In Fig. 6, the reflection losses within the 0.1–20 GHz frequency range were calculated using five intelligent algorithms. After comprehensive comparison, HSEAO can cover the vast majority of bandwidths from 0.1 to 20 GHz, with only suboptimal performance in the 0.1 to 2.31 GHz band.

As shown in Fig. 7, HSEAO achieves superior convergence accuracy in the later stages compared to EAO. This enhanced performance demonstrates that the algorithm's improvements effectively prevent convergence in local optima.

4.2.3. Validation of Simulation Results Using CST

The Computer Simulation Technology (CST) Microwave Studio Suite (MWS), a widely used tool for electromagnetic simulation, was employed to validate the effectiveness of various MMA designs [22, 23]. In this study, all simulations were conducted using CST's Finite Element Method (FEM) solver operating in the frequency domain.

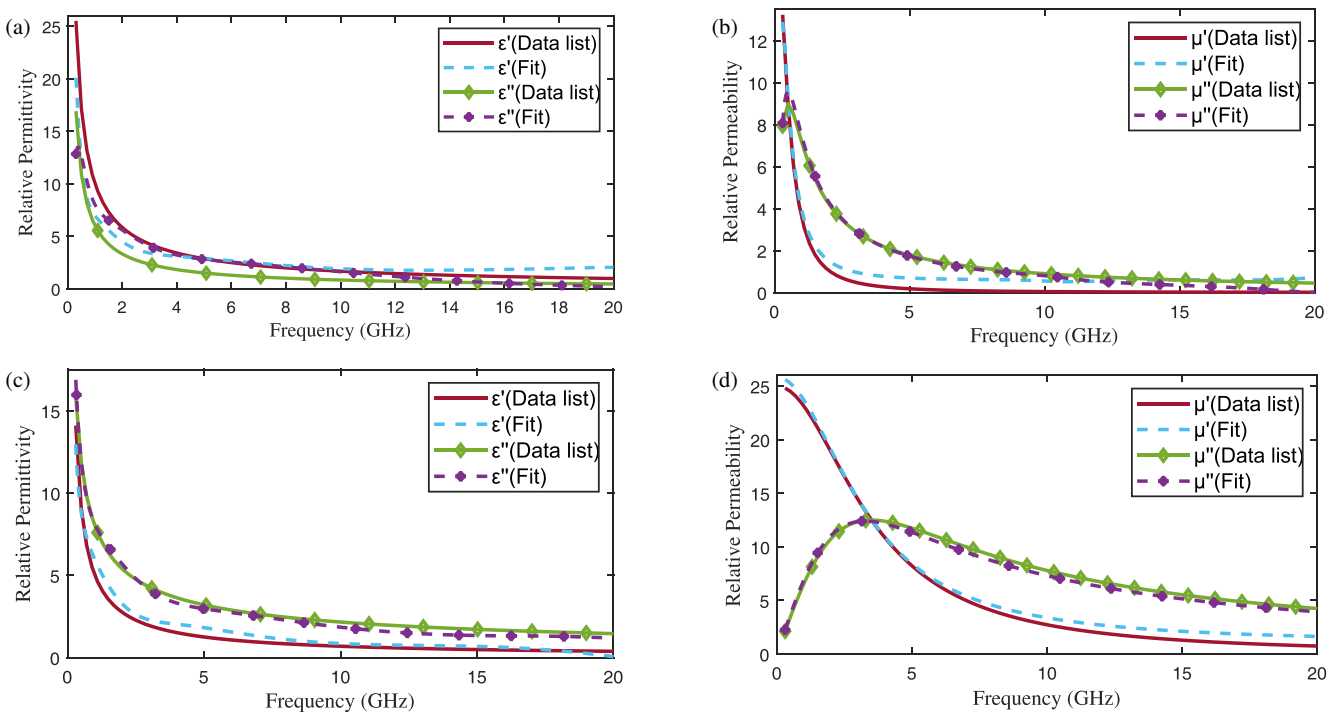

FIGURE 8. Comparison of the supplied and fitted material dispersion curves in CST: (a) Material 8, (b) Material 12, (c) Material 6, and (d) Material 16.

TABLE 1. Parameters of relative absorbing materials.

Lossless dielectric materials ($\mu' = 1, \mu'' = 0$)				
#	ε'			
1	10			
2	50			
Lossy magnetic materials ($\varepsilon' = 15, \varepsilon'' = 0$) $\mu = \mu' - j\mu''$, $\mu'(f) = \frac{\mu'(1\,\text{GHz})}{f^a}$, $\mu''(f) = \frac{\mu''(1\,\text{GHz})}{f^b}$				
#	$\mu'(1\,\text{GHz})$	a	$\mu''(1\,\text{GHz})$	b
3	5	0.974	10	0.961
4	3	1	15	0.957
5	7	1	12	1
Lossy dielectric materials ($\mu' = 1, \mu'' = 0$) $\varepsilon = \varepsilon' - j\varepsilon''$, $\varepsilon'(f) = \frac{\varepsilon'(1\,\text{GHz})}{f^a}$, $\varepsilon''(f) = \frac{\varepsilon''(1\,\text{GHz})}{f^b}$				
#	$\varepsilon'(1\,\text{GHz})$	a	$\varepsilon''(1\,\text{GHz})$	b
6	5	0.861	8	0.569
7	8	0.778	10	0.682
8	10	0.778	16	0.861
Relaxation-type magnetic materials ($\varepsilon' = 15, \varepsilon'' = 0$) $\mu'(f) = \frac{\mu_m f_m^2}{f^2+f_m^2}$, $\mu''(f) = \frac{\mu_m f_m f}{f^2+f_m^2}$ f and f_m in GHz				
#	μ_m		f_m	
9	35		0.8	
10	35		0.5	
11	30		1.0	
12	18		0.5	
13	20		1.5	
14	30		2.5	
15	30		2.0	
16	25		3.5	

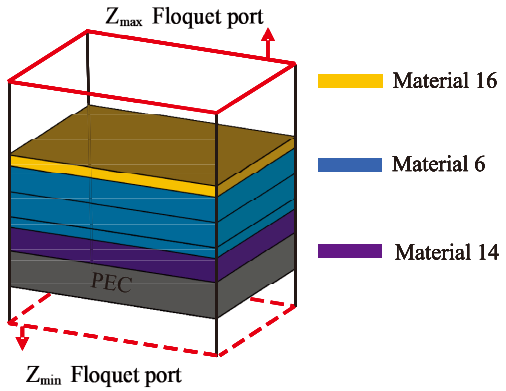

FIGURE 9. Model in CST.

Materials 3 through 16 in Table 1 were imported into the CST material database. CST Studio employs fitting techniques internally to store externally provided material property parameters. Due to the presence of material dispersion types, this fitting process introduces errors between the original data and fitted results, leading to deviations between CST simulation outcomes and calculated results. Fitted data for Materials 8, 12, 6, and 16 are provided in Fig. 8. Among these materials, Materials 8 and 12 exhibit relatively large fitting errors [24].

The model of MMA was constructed in CST, with the material types and thicknesses of each layer matching the optimized data obtained from HSEAO in MATLAB. The simulation treats the absorber structure as an infinitely periodic array, with repetition occurring along the x and y directions. Two Floquet ports are placed at the upper and lower limits to facilitate the simulation of wave incidence and reflection. The incident angle of the plane wave is set to 0 degrees. The frequency range for the

TABLE 2. Comparison of optimal optimization results for five-layer microwave absorbers.

Algorithm	HSEAO		EAO		BLSA-SA		DE		BESOA	
Layers	Type	Thickness	Type	Thickness	Type	Thickness	Type	Thickness	Type	Thickness
1	16	0.37698	16	0.3719	16	0.3682	16	0.384	16	0.417
2	6	1.4183	6	1.6973	6	1.958	6	0.433	6	1.109
3	6	1.4853	7	1.2822	6	1.1016	6	1.143	6	1.7883
4	6	0.34023	16	0.92828	14	0.4834	6	1.446	3	0.2146
5	14	1.3551	13	0.87122	15	0.9424	15	1.454	15	1.2711
Total thickness (mm)	4.97591		4.99354		4.8536		4.86		4.8	
Max. reflection loss (dB)	-25.7975		-24.0352		-25.8528		-25.485		-25.765	
Avg. reflection loss (dB)	-28.6851		-26.3872		-27.8752		-27.8292		-27.7014	

TABLE 3. Comparison of optimal optimization results for seven-layer microwave absorbers.

Algorithm	HSEAO		EAO		DE		BLSA-SA		CSA	
Layers	Type	Thickness	Type	Thickness	Type	Thickness	Type	Thickness	Type	Thickness
1	16	0.213	16	0.20365	14	0.2064	16	0.208	14	0.2107
2	6	2.0125	6	1.4286	6	1.8762	6	1.749	6	1.1066
3	14	0.61419	14	0.38127	16	0.5391	16	0.085	16	0.7916
4	7	0.88176	5	0.74152	6	0.9499	6	0.082	6	0.5482
5	5	0.92015	5	0.75971	5	1.9596	14	0.4922	5	1.3785
6	5	1.9074	4	0.50543	4	0.7817	5	1.502	4	0.557
7	4	0.4608	4	1.0305	5	0.4864	4	1.6602	5	1.745
Total thickness (mm)	6.7993		5.05068		6.7993		5.7784		6.3376	
Max. reflection loss (dB)	-18.1965		-16.5045		-17.9		-18.0406		-18.0879	
Avg. reflection loss (dB)	-19.6419		-17.9992		-19.1169		-19.2074		-19.5157	

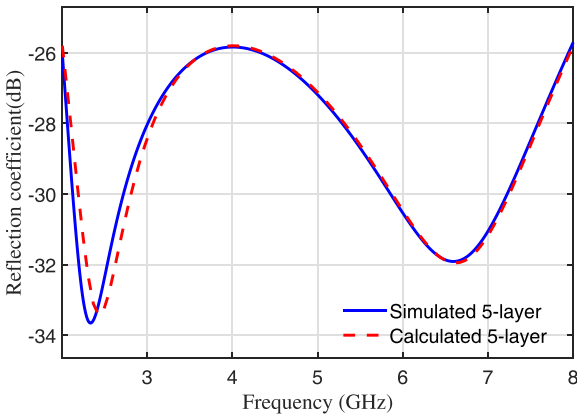

FIGURE 10. Comparison of reflection coefficients obtained via HSEAO optimization and CST simulation in the five-layer structure.

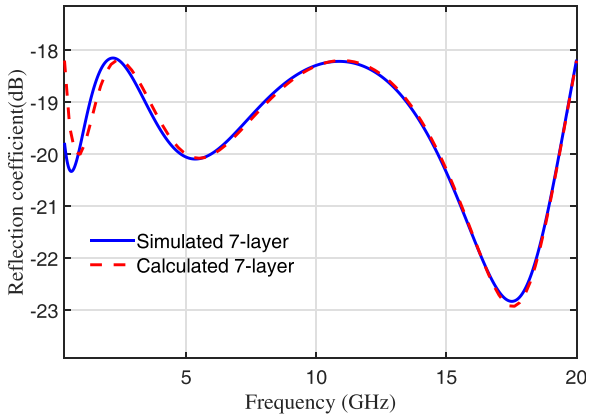

FIGURE 11. Comparison of reflection coefficients obtained via HSEAO optimization and CST simulation in the seven-layer structure.

five-layer absorber is set to 2–8 GHz, and the frequency range for the seven-layer absorber is set to 0.1–20 GHz. Using these settings consistent with the physical model, construct a plane wave model in CST, as shown in Fig. 9.

The reflection coefficient curves of the optimized designs for the five-layer and seven-layer structures are shown in Figs. 10 and 11. These results indicate that there is no significant difference between the numerical calculation results and the electromagnetic simulation results. This confirms the reliability of the mathematical model and the effectiveness of the optimization algorithm used for the MMA.

5. CONCLUSION

This study introduces Hybrid Multi-Strategy Enhanced Enzyme Action Optimizer (HSEAO), which incorporates three distinct improvement strategies to enhance the design of multilayer microwave absorbers (MMA) under normal incidence. The proposed method effectively identifies coating configurations that minimize the magnitude of the reflection coefficient within a specified frequency band and total thickness constraint. For performance verification, two absorber models were designed. In the five-layer structure operating over 2–8 GHz, the HSEAO-optimized design achieved maximum and average reflection losses of -25.80 dB and -28.69 dB, respectively. For the seven-layer configuration covering 0.1–20 GHz, the optimized model attained reflection losses of -18.20 dB and -19.64 dB, respectively. The obtained results were compared with those of several optimization algorithms reported in the literature. In both cases, HSEAO consistently produced lower peak and average reflection losses than the competing methods, confirming the effectiveness of the proposed enhancements and the strong optimization capability of HSEAO.

These results not only verify the effectiveness of the improved approach and the robust optimization capability of HSEAO, but also demonstrate its potential for practical engineering applications. The proposed broadband and high-efficiency absorber structure can greatly enhance the electromagnetic stealth performance of targets. In addition, in electromagnetic compatibility (EMC) applications, such low-reflection coatings effectively suppress electromagnetic interference. The validation of this study is primarily conducted through CST simulations. In this work, 16 synthetic materials were utilized to design multilayer microwave absorbers. Future research will further expand the material library by incorporating novel practical absorptive materials, thereby enabling more advanced MMA designs using HSEAO.

ACKNOWLEDGEMENT

This work is supported by the China Postdoctoral Science Foundation (Grant No. 2025M770506), the School-Level Research Projects of Yancheng Institute of Technology (Grant No. xjr2024038 and Grant No. xjr2024036), the College Students Innovation and Entrepreneurship Training Program (Grant No. 2025482 and No. 2025518), the Natural Science Research Project of Jiangsu Higher Education Institutions (Grant No. 24KJB510051 and Grant No. 24KJB140020).

REFERENCES

[1] Pang, H., Y. Duan, L. Huang, L. Song, J. Liu, T. Zhang, X. Yang, J. Liu, X. Ma, J. Di, and X. Liu, "Research advances in composition, structure and mechanisms of microwave absorbing materials," *Composites Part B: Engineering*, Vol. 224, 109173, 2021.

[2] Panwar, R. and J. R. Lee, "Recent advances in thin and broadband layered microwave absorbing and shielding structures for commercial and defense applications," *Functional Composites and Structures*, Vol. 1, No. 3, 032001, 2019.

[3] Panwar, R., S. Puthucheri, D. Singh, and V. Agarwala, "Design of ferrite-graphene-based thin broadband radar wave absorber for stealth application," *IEEE Transactions on Magnetics*, Vol. 51, No. 11, 1–4, 2015.

[4] Razek, A., "Assessment of a functional electromagnetic compatibility analysis of near-body medical devices subject to electromagnetic field perturbation," *Electronics*, Vol. 12, No. 23, 4780, 2023.

[5] Peng, T., C. Zhu, T. Zhou, B. Zhang, D. Ye, X. Li, and L. Ran, "A compact microwave imager integrated with a miniaturized dual-angle anechoic chamber," *IEEE Transactions on Microwave Theory and Techniques*, Vol. 69, No. 11, 4831–4839, 2021.

[6] Vidaković, M. and D. Vinko, "Hardware-based methods for electronic device protection against invasive and non-invasive attacks," *Electronics*, Vol. 12, No. 21, 4507, 2023.

[7] Michielssen, E., J.-M. Sajer, S. Ranjithan, and R. Mittra, "Design of lightweight, broad-band microwave absorbers using genetic algorithms," *IEEE Transactions on Microwave Theory and Techniques*, Vol. 41, No. 6, 1024–1031, 1993.

[8] Roy, S., S. D. Roy, J. Tewary, A. Mahanti, and G. Mahanti, "Particle swarm optimization for optimal design of broadband multilayer microwave absorber for wide angle of incidence," *Progress In Electromagnetics Research B*, Vol. 62, 121–135, 2015.

[9] Chamaani, S., S. A. Mirtaheri, and M. A. Shooredeli, "Design of very thin wide band absorbers using modified local best particle swarm optimization," *AEU — International Journal of Electronics and Communications*, Vol. 62, No. 7, 549–556, 2008.

[10] Dib, N. I., M. Asi, and A. Sabbah, "On the optimal design of multilayer microwave absorbers," *Progress In Electromagnetics Research C*, Vol. 13, 171–185, 2010.

[11] Roy, S., A. Mahanti, S. D. Roy, and G. K. Mahanti, "Comparison of evolutionary algorithms for optimal design of broadband multilayer microwave absorber for normal and oblique incidence," *Applied Computational Electromagnetics Society Journal (ACES)*, Vol. 31, No. 1, 79–84, 2021.

[12] Lu, Y. and Y. Zhou, "Design of multilayer microwave absorbers using hybrid binary lightning search algorithm and simulated annealing," *Progress In Electromagnetics Research B*, Vol. 78, 75–90, 2017.

[13] Kankılıç, S. and E. Karpat, "Optimization of multilayer absorbers using the bald eagle optimization algorithm," *Applied Sciences*, Vol. 13, No. 18, 10301, 2023.

[14] Zong, Y. M., W. B. Kong, J. P. Li, L. Wang, H. N. Zhang, F. Zhou, and Z. Y. Cheng, "Optimization of multilayer microwave absorbers using multi-strategy improved gold rush optimizer," *Applied Computational Electromagnetics Society Journal (ACES)*, Vol. 39, No. 8, 708–717, 2024.

[15] Liu, S., Y. Zhang, H. Wang, F. Wu, S. Tao, and Y. Zhang, "Efficient design of broadband and low-profile multilayer absorbing materials on cobalt-iron magnetic alloy doped with rare earth element," *Nanomaterials*, Vol. 14, No. 13, 1107, 2024.

[16] Wang, T., G. Chen, J. Zhu, H. Gong, L. Zhang, and H. Wu, "Deep understanding of impedance matching and quarter wavelength theory in electromagnetic wave absorption," *Journal of Colloid and Interface Science*, Vol. 595, 1–5, 2021.

[17] Toktas, A., D. Ustun, and M. Tekbas, "Multi-objective design of multi-layer radar absorber using surrogate-based optimization," *IEEE Transactions on Microwave Theory and Techniques*, Vol. 67, No. 8, 3318–3329, 2019.

[18] Rodan, A., A.-K. Al-Tamimi, L. Al-Alnemer, S. Mirjalili, and P. Tiňo, "Enzyme action optimizer: A novel bio-inspired optimization algorithm," *The Journal of Supercomputing*, Vol. 81, No. 5, 686, 2025.

[19] Wang, Z., L. Huang, S. Yang, D. Li, D. He, and S. Chan, "A quasi-oppositional learning of updating quantum state and Q-learning based on the dung beetle algorithm for global optimiza-

tion," *Alexandria Engineering Journal*, Vol. 81, 469–488, 2023.

[20] Wang, S., G. Liu, M. Gao, S. Cao, A. Guo, and J. Wang, "Heterogeneous comprehensive learning and dynamic multi-swarm particle swarm optimizer with two mutation operators," *Information Sciences*, Vol. 540, 175–201, 2020.

[21] Ghasemi, M., M. Deriche, P. Trojovský, Z. Mansor, M. Zare, E. Trojovská, L. Abualigah, A. E. Ezugwu, and S. K. Mohammadi, "An efficient bio-inspired algorithm based on humpback whale migration for constrained engineering optimization," *Results in Engineering*, Vol. 25, 104215, 2025.

[22] Yao, H., J. Yang, H. Li, J. Xu, and K. Bi, "Optimal design of multilayer radar absorbing materials: A simulation-optimization approach," *Advanced Composites and Hybrid Materials*, Vol. 6, No. 1, 43, 2023.

[23] Yigit, E. and H. Duysak, "Determination of optimal layer sequence and thickness for broadband multilayer absorber design using double-stage artificial bee colony algorithm," *IEEE Transactions on Microwave Theory and Techniques*, Vol. 67, No. 8, 3306–3317, 2019.

[24] Warhekar, P., A. Bhattacharya, and S. Neogi, "Designing thinner broadband multilayer radar absorbing material through novel formulation of cost function," *IEEE Access*, Vol. 11, 91 016–91 027, 2023.